LBL-17657 c.2
UC-21

Lawrence Berkeley Laboratory

UNIVERSITY OF CALIFORNIA

RECEIVED
LAWRENCE
BERKELEY LABORATORY

JUN 15 1984

LIBRARY AND
DOCUMENTS SECTION

Accelerator & Fusion Research Division

HEAVY ION FUSION HALF-YEAR REPORT
October 1, 1983 - March 31, 1984

Heavy Ion Fusion Staff

April 1984

TWO-WEEK LOAN COPY

This is a Library Circulating Copy which may be borrowed for two weeks. For a personal retention copy, call Tech. Info. Division, Ext. 6782.

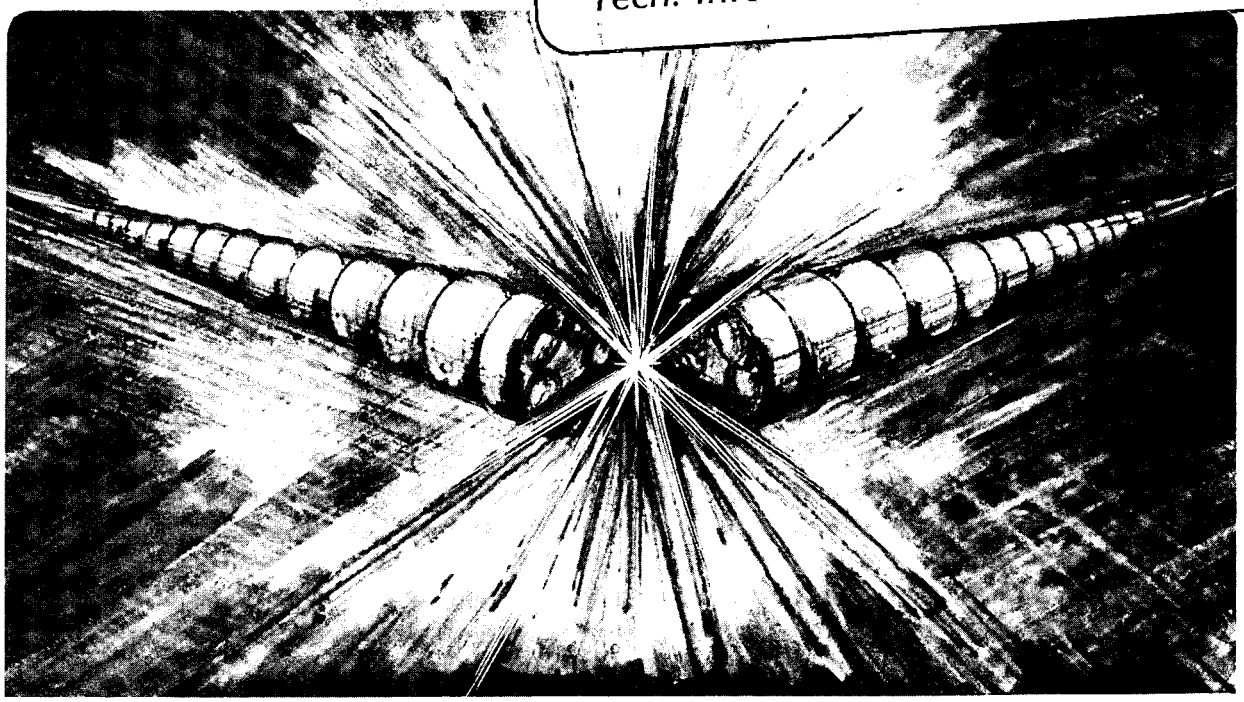

Prepared for the U.S. Department of Energy under Contract DE-AC03-76SF00098

LBL-17657 c.2

DISCLAIMER

This document was prepared as an account of work sponsored by the United States Government. While this document is believed to contain correct information, neither the United States Government nor any agency thereof, nor the Regents of the University of California, nor any of their employees, makes any warranty, express or implied, or assumes any legal responsibility for the accuracy, completeness, or usefulness of any information, apparatus, product, or process disclosed, or represents that its use would not infringe privately owned rights. Reference herein to any specific commercial product, process, or service by its trade name, trademark, manufacturer, or otherwise, does not necessarily constitute or imply its endorsement, recommendation, or favoring by the United States Government or any agency thereof, or the Regents of the University of California. The views and opinions of authors expressed herein do not necessarily state or reflect those of the United States Government or any agency thereof or the Regents of the University of California.

LBL-17657
HI-FAN-249

HEAVY ION FUSION HALF-YEAR REPORT*

October 1, 1983 - March 31, 1984

Heavy Ion Fusion Staff

Accelerator and Fusion Research Division

Lawrence Berkeley Laboratory
University of California
Berkeley, California 94720

April 1984

Attention: This document is provided for DOE "Official Use". Distribution to other interested parties is made with the understanding that no information or experimental results, given herein, will be quoted without first obtaining the authors' permission, or until such information or results have appeared in the open literature.

*This work was supported by the Office of Energy Research, Office of Basic Energy Sciences, U.S. Department of Energy under Contract No. DE-AC03-76SF00098.

CONTENTS

	Page
HIGHLIGHTS	1
SINGLE BEAM TRANSPORT EXPERIMENT	3
1. Introduction	3
2. Gas Attenuation in SBTE: Measurement of Charge Exchange Cross Sections	4
3. Time of Flight Measurements	5
4. Instabilities and Stability Limits	5
BEAM DIAGNOSTICS DEVELOPMENT	11
1. Automated 2-Slit Scan	11
2. Optical Multichannel Analyzer with Scintillator and Pepper Shaker	11
THE NEUTRALIZED BEAM FOCUSING EXPERIMENT	14
INDUCTION LINAC COMPONENT DEVELOPMENT	17
1. 200 kV Test Stand	17
2. Insulator Development	17
2.1. Polysil Model Insulators	17
2.2. Re-X Insulator	18
3. MBE Electrostatic Quadrupole Array	20
4. Outgassing Measurements	24
5. Switch Tube Development	24
6. Metglas Core Tests	25
7. Surface Ionization Sources	26
MULTIPLE BEAM EXPERIMENT (MBE)	29

Page

THEORY 32

1. Design Questions for MBE 32

2. Calculation of Non K-V Equilibrium Properties 36

PUBLICATIONS 38

H.I.F. STAFF ROSTER 40

DISTRIBUTION LIST 41

HIGHLIGHTS

1. The "INS International Symposium on Heavy Ion Accelerators and Their Applications to Inertial Fusion" took place at Tokyo in January 1984 and significant results of the LBL research and development were reported there.

2. Results from the Single Beam Transport Experiment (SBTE), reported at Tokyo, showed that stable beam transport in a 41-period AG lattice with single-particle phase advance per period, $\sigma_0 = 60^\circ$, was possible with space-charge forces large enough to depress the phase-advance to $\sigma = 12^\circ$. We have since extended that result and have shown that depression from $\sigma_0' = 60^\circ$ to $\sigma = 8^\circ$ is still stable.

3. Measurements of the Cs^+ ion beam attenuation in the SBTE at different gas pressures, taken together with the different lattice acceptances for singlyand doubly-charged ions, have allowed us to measure <u>both</u> the electron pick-up and electron loss cross-sections for Cs^+ on nitrogen at 160 keV.

4. A large effort is under way to arrive at a conceptual reference design for the Multiple Beam Experiment (MBE), so that final engineering design and prototyping can begin as soon as possible. Questions such as quadrupole dimensions, alignment tolerances (both from lens to lens within a single array, and from array to array), support, survey and alignment systems, insulator configuration, and the packing of the cores and modules, are all under intensive study.

5. The MBE design process has stimulated many detailed questions for the theory group and several important results have ensued. For instance, on the question of what magnitude of sextupole component could be tolerated in the lenses, computer simulation showed that, for a space-charge-dominated beam, a significant sextupole term had essentially no effect if the beam remained on axis, but led to intolerable emittance growth for the practical case of an off-axis beam.

SINGLE BEAM TRANSPORT EXPERIMENT

1. Introduction

The Single Beam Transport Experiment is intended to investigate the long term stability of heavily space-charge loaded ion beam transport in an alternating gradient lattice, with the goal of characterizing stability thresholds and instability modes. The threshold information is of immediate interest in the optimization of the accelerator design for the proposed High Temperature Experiment, as well as for longer term heavy ion beam-driven fusion development. The relevant parameters are the single particle phase advance per focusing period (σ_0) and the space-charge reduced phase advance (σ). As current density increases, σ falls toward zero. However, there is no experimental knowledge of whether a limit on σ exists for stable transport (as conjectured by Maschke and as suggested by the idealized KV distribution function).

In reporting on experimental data it is important to define the prescription whereby a value of phase advance is derived. The zero-current phase advance, σ_0, is accurately arrived at by calculation from the quadrupole fields. To derive σ, the measured rms emittance (multiplied by four) together with the measured beam current, are used in an "equivalent KV" envelope calculation to derive a numerical value of σ. Such a definition corresponds to an rms σ rather than a small-amplitude σ appropriate to an exact KV envelope calculation.

As of September, 1983, we had 82 electrostatic transport quadrupoles with uniform voltages after 5 matching quadrupoles so powered as to match the azimuthally symmetric gun output beam into the A.G. lattice. Diagnostics included a shallow gridded Faraday cup near the gun, a deep gridless cup at

the end of the lattice, and slits for measuring the emittance (the distribution of particles as a function $f(x,x')$, where x is a transverse dimension). We also had installed a set of control grids just downstream of the gun to raise the emittance, and also a varaible attenuator to make possible a less intense beam for measurement and comparison.

We have carried out most of the calibration and exploratory program required and have completed much of the planned exhaustive cataloging of beam behavior as a function of σ_0 and σ [see sub-section 4 below].

2. Gas Attenuation in SBTE: Measurement of Charge Exchange Cross Sections

Using a small-diameter, low-current beam ($\sigma \sim \sigma_0$) for which there was a large aperture clearance, we measured the current transmitted to the lattice end as a function of gas pressure and σ_0. The beam was matched for $\sigma_0 = 60°$, with σ near 50°, and measurements of current covered the range of σ_0 for which the beam passed through the lattice without intercepting the quadrupoles, no adjustments being made to match it at other σ_0 settings. At the base pressure for these measurements (4×10^{-7} Torr indicated), the current varied by only 1-2 percent over a large range of σ_0, dropping only when mismatched so badly that the bulk beam intercepted the quads. Higher pressures were obtained with a leak valve connected to open atmosphere.

The total effective cross-sections for neutralization and second ionization (resp., σ_{10} and σ_{12}) can be separately derived since, for low-σ_0 lattices ($\sigma_0(Cs^{+1}) \lesssim 60°$, corresponding to $\sigma_0(Cs^{+2}) \lesssim 180°$), the Cs^{+2} ions formed are also stably transported in the lattice, while for stronger lenses the Cs^{+2} ions are unstable and, hence, lost. When the Cs^{+2} is

also transported, the current at the end of the lattice increases by an amount proportional to $\sigma_{12}\,\sigma_{10}$ but, when both Cs^{+2} and Cs^{0} are lost, it decreases in proportion to $\sigma_{12} + \sigma_{10}$. The results, shown in Fig. 1, for 160 kV Cs^{+} ions, give approximate values of $\sigma_{12} \approx \sigma_{10} \approx 5\times10^{-16}\,cm^{2}$, the target gas being presumably N_2, the predominant gas in the air leak. This implies that for our 13 m long system the effect of charge-exchange collisions with background gas will be in the 1-2 percent range if the indicated pressure is in the few times 10^{-7} Torr range. The effect of image forces on an intense beam can be at this same level for moderate to large aperture fill factors.

3. Time of Flight Measurements

We used the time of flight for the beam between two Faraday cups to cross-calibrate our electrical measurement of gun voltage, obtaining 158 kV ±2 percent versus an electrical measurement of 160 kV ±1 percent. The time of flight also allowed us to characterize the mass species of the light contaminants of our beam (total < 4 percent). We found mass numbers corresponding to all fragments of Al_2O_3 and SiO_2, and perhaps potassium. There is a time lag between the start of Cs^{+} emission and the light fractions of 200-300 ns, which is just the time required for the Cs^{+} to get to the grid at the gun end. This indicates that the light ions might be decomposition products from e^{-} back-bombardment of the source from the grid.

4. Instabilities and Stability Limits

Envelope instabilities occur for settings of the focussing strength above $\sigma_0 = 90^\circ$ and for relatively small transported currents. The threshold current (as measured by σ) for onset of instability was explored as follows.

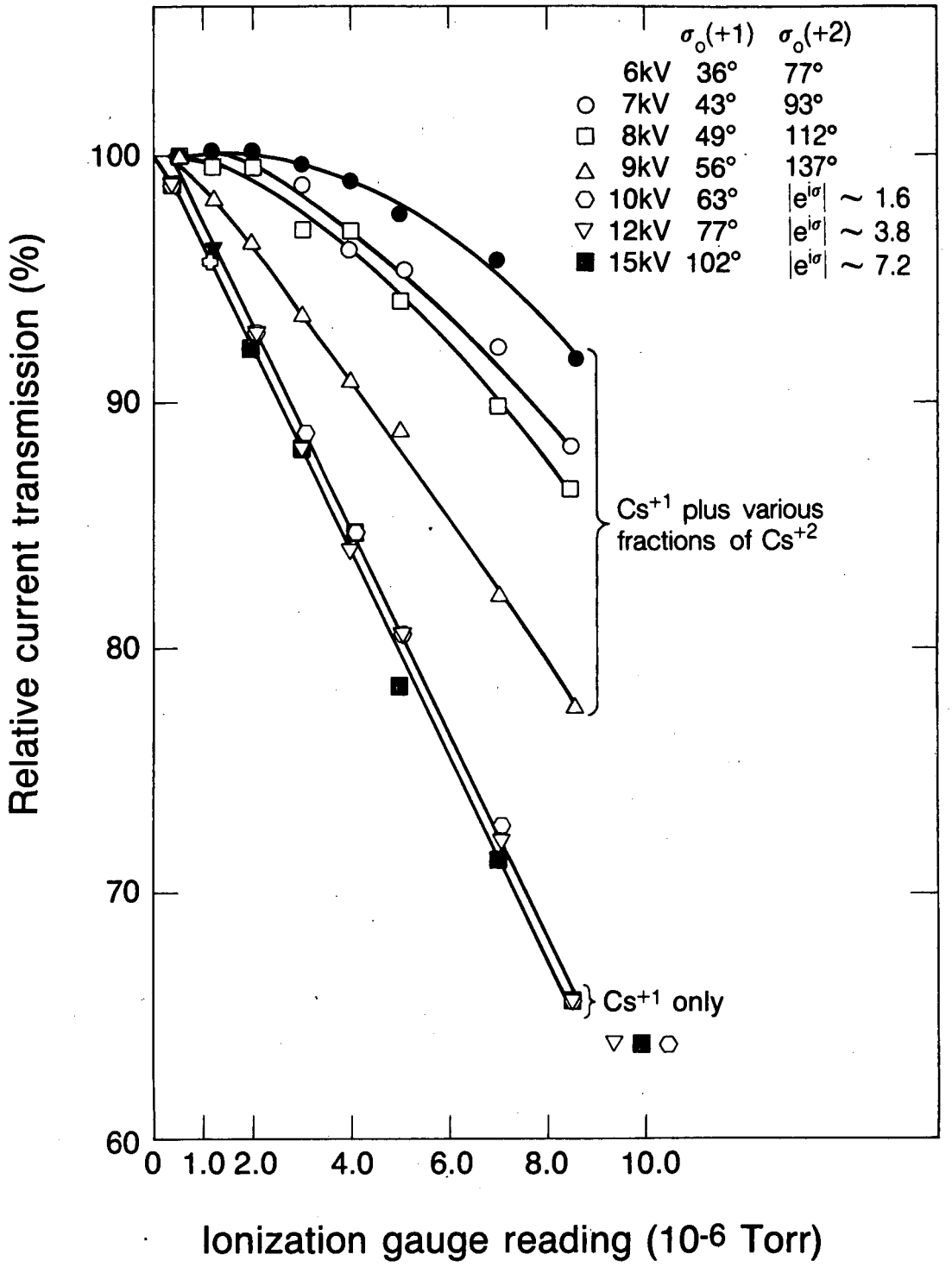

XBL 844-10465

Fig. 1. Relative current transmitted through 87 quadrupoles as a function of pressure at various voltage settings of the last 82 quadrupoles. Constant I vs. p for V_Q = 10 kV to V_Q = 15 kV indicates no beam loss due to aperture limits. The 6 kV line initial slope of zero implies charge exchange cross sections to Cs^0 and Cs^{+2} are nearly equal. Calculated Cs^{+2} ion acceptance falls to zero at $\gtrsim$ 10 kV.

By using 3.4 mA of beam current and applying a variable voltage to the emittance control grids, we measured the output emittance vs. input emittance for beams initially matched into a $\sigma_0 = 120^\circ$ lattice. Changing ε for a fixed σ_0 and fixed current I, has the effect of changing σ which depends on ε as well as I. [Experimentally, it is easier to set I and scan σ by varying ε rather than changing I at fixed ε.] Figure 2 shows the sharp threshold for emittance growth near $\sigma \sim 95^\circ$ (calculated from I,ε) and is given here as just one example of the type of threshold measurement we are making, though for $\sigma_0 \sim 90^\circ$ the effect is not nearly as dramatic. This example is an extension of the 120° measurement reported in the FY 1983 year-end report.

Another experiment made was to shadow out a slice of the beam in physical space with a wire and measure the rotation of the shadow in the (x,x') plot to derive an independent estimate of the depressed phase advance, σ. Various systematics make the measurement difficult to interpret accurately, but the measurements done so far give good agreement with the calculated $\sigma(\varepsilon,I)$, as described earlier in sub-section 1.

In an attempt to investigated beam behavior beyond the $60^\circ \gtrsim 12^\circ$ result quoted last reporting period, we raised the current from the injector by shortening the gun structure. Unfortunately, non-thermal effects cause our beam emittance to be 5-6 times thermal estimates based on source temperature, and these effects scale so as to cancel part of the gain we made in current. They cause the unnormalized emittance of the beam to be roughly independent of gun voltage for a given geometry, and since the depressed σ depends on the ratio of the unnormalized emittance to the gun perveance, changing the gun voltage and quadrupole settings together results in little change in σ. The new values of current and normalized emittance at 160 kV are 23 mA and

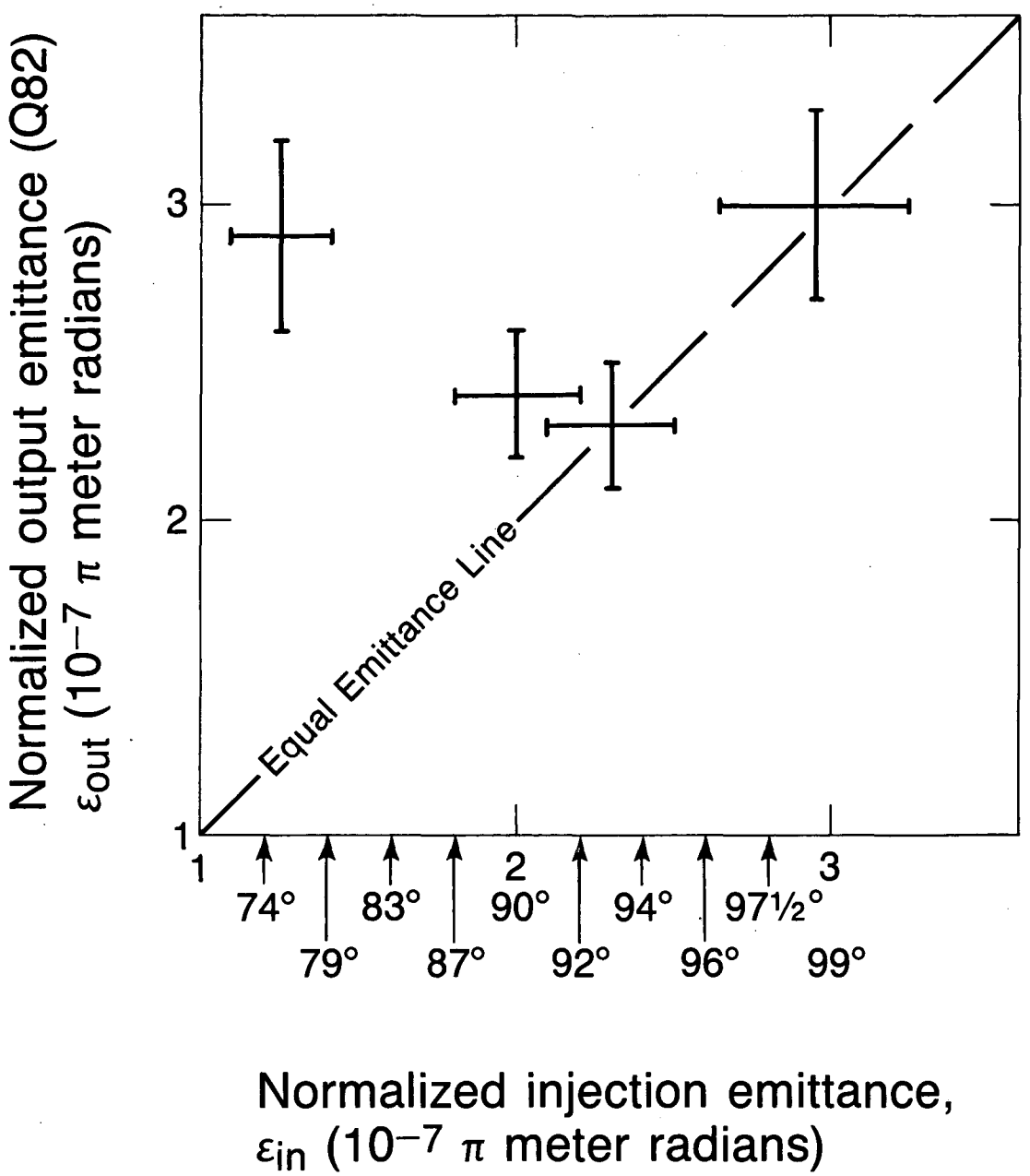

XBL 844-10466

Fig. 2. Measured output emittance 80 quadrupoles downstream from input emittance measurement for 3.45 mA Cs^+ beam at 160 kV with $\sigma_0 \sim 120°$. Approximate depressed tune (σ) values for injection emittance are shown on horizontal axis.

$\varepsilon \sim 1.6\times10^{-7}\ \pi$ meter radian. We have used a beam energy of 120 kV since January to avoid drawing too much current from our gun, which could cause depletion of the surface Cs layer. (This effect was seen on our older source with 6 months of service when used in the shorter gun at 160 kV, but not on the new one we installed in January 1984.) For stable propagation of a Cs^{+1} beam with 120 kV energy, at 15.2 mA, and $\varepsilon_N = 1.4\times10^{-7}\ \pi$ meter-radians and $\sigma_0 = 60^\circ$, we have achieved a value of $\sigma \approx 8^\circ$.

We have added the capability to measure beam emittance (horizontal only) at Q35 and Q59 of the 82 quadrupole array, and have also installed shallow Faraday cups after Q36 and Q60. In addition, we have improved all of our emittance scanning equipment to allow measurement of the entire (x,x') phase plane, well into the wings of the distribution. These diagnostics are now being used to monitor the emittance and current along the transport lattice.

We have implemented an automatic data scanning system to allow detailed scanning of the density distribution $f(x,x')$. The data generated are stored on magnetic media to aid later analysis and graphical presentation. Some preliminary examples of this are shown in Fig. 3, though the analysis is not yet complete.

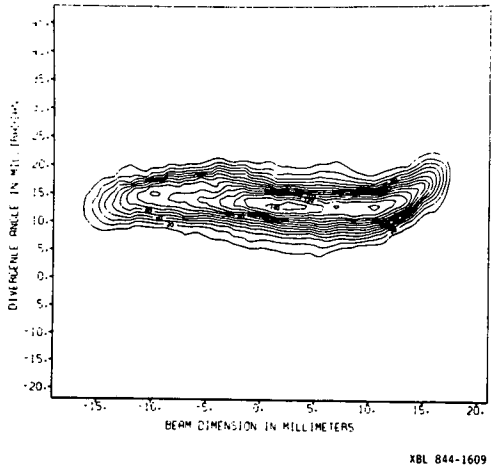

60° lattice, Q4 Horizontal (beginning)

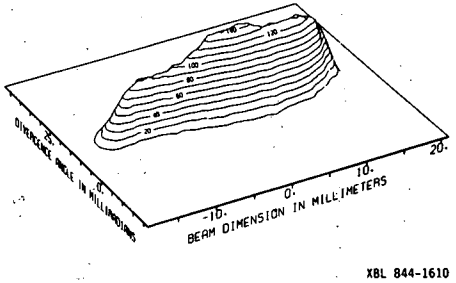

→ **perspective view**

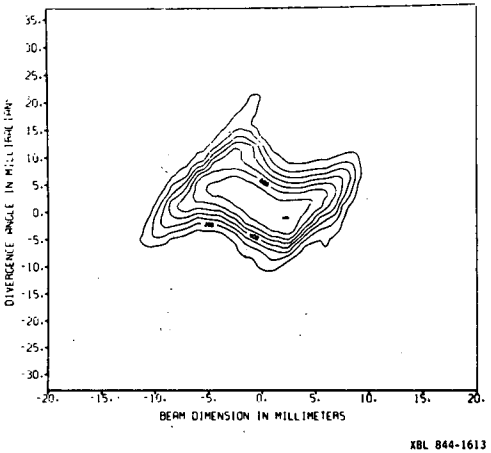

80° lattice, Q4 Horizontal (beginning)

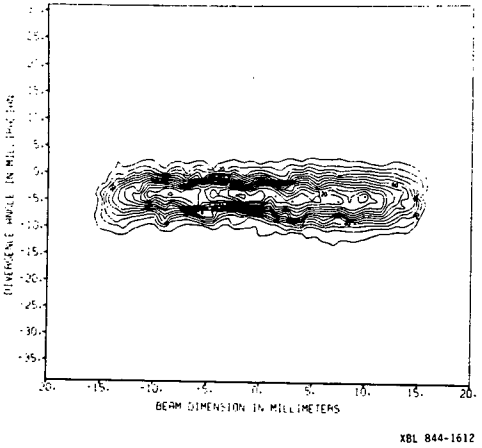

60° lattice, Q80 Horizontal (end)

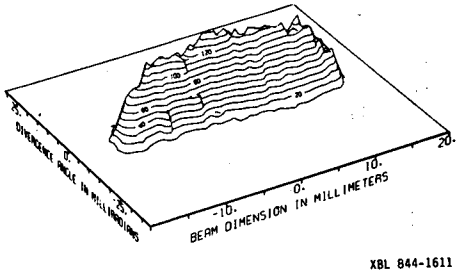

→ **perspective view**

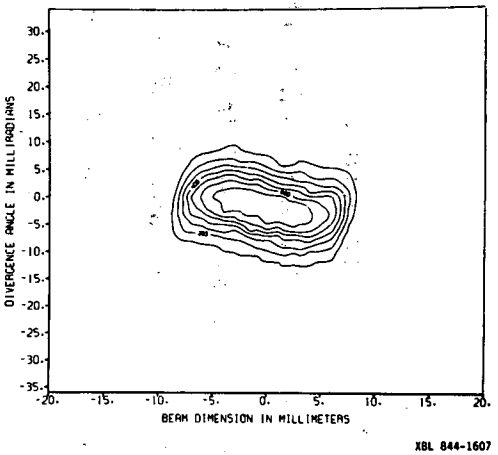

80° lattice, Q80 Horizontal (end)

Fig. 3. The above labeled figures are meant to provide examples of the type of data obtainable from the Single Beam Transport Experiment. The contours are equally spaced, but have no relationship to the proportion of beam contained inside the contours, so that relative emittances may not be compared in detail. However, the general shapes of the contours are significant.

BEAM DIAGNOSTICS DEVELOPMENT

1. Automated 2-Slit Scan

In order to speed up the measurement of emittance, a system has been designed and built to control the positions of two narrow slits displaced longitudinally from one another in an intense Cs^+ beam. The current passing through the slits is detected by a large Faraday cup whose signal is acquired by a digital storage oscilloscope. The slits are moved by stepping motors. The entire system is driven under program control by a desktop computer (HP-85) which plots and prints the beam profile and transverse emittance data on its internal printer. A valuable feature of this computer control is the ability to acquire the emittance plot quickly by calculating the expected position of the final three points from the values obtained for the first two points. This reduces the real time required to acquire the data.

This system was run successfully on the SBTE, automatically acquiring and plotting a phase plot in 22 minutes, which is four times faster than the previous manual method. The work has been written up as an internal report, LBID-880.

2. Optical Multichannel Analyzer with Scintillator and Pepper Shaker

Because the EG and G Optical Multichannel Analyzer (OMA) has the capability of acquiring a two-dimensional image of a Cs beam on a $CaF_2(Eu)$ scintillator we have constructed a "pepper shaker," shown in Fig. 4(a) which was installed in the midplane between Q80 and Q81 on the SBTE. A photograph of the transmitted beam on a scintillator between Q81 and Q82 is shown in

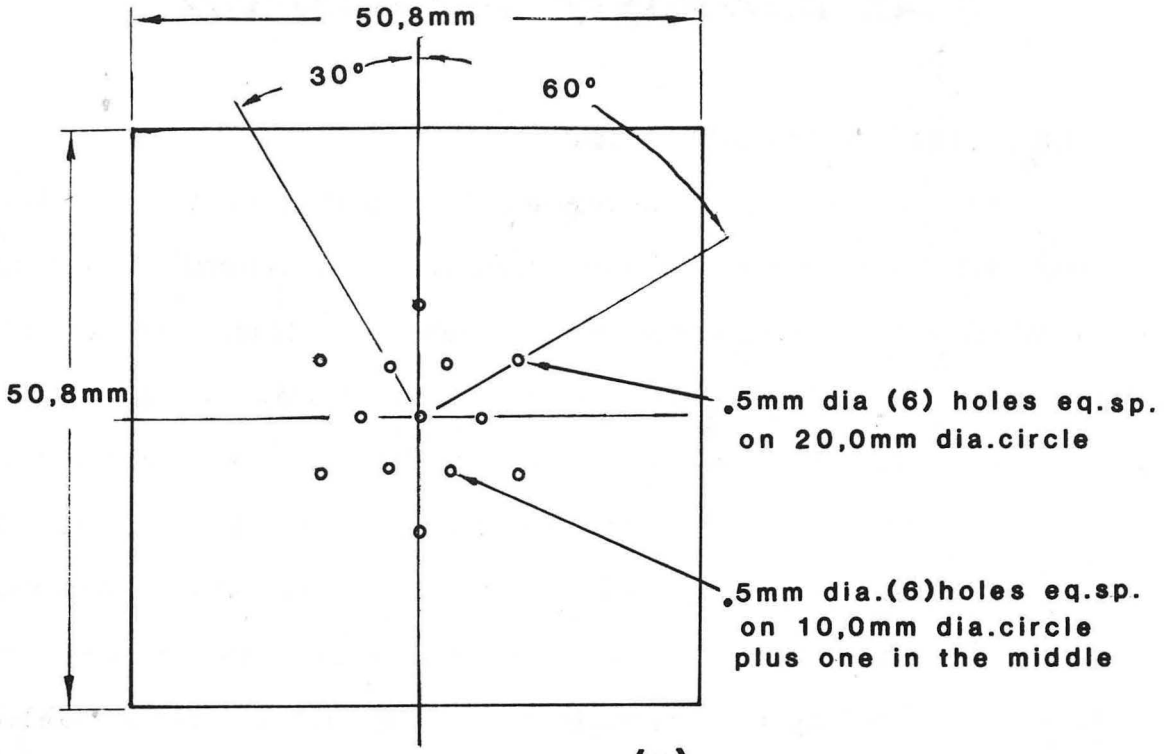

(a)

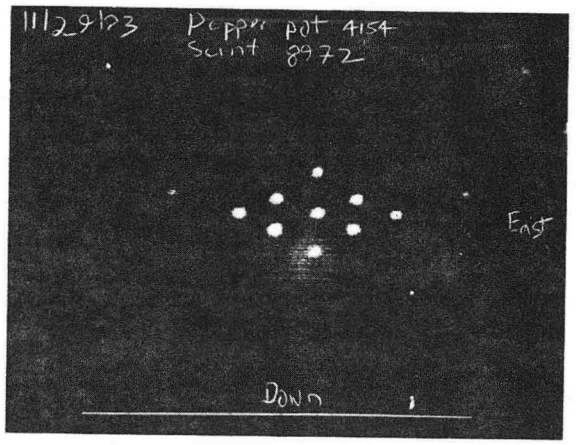

(b)

XBB 844-2954

Fig. 4(a) Sketch of the "pepper pot" used with OMA-scintillator system on SBTE drawn to same scale as photograph.

(b) Photograph of OMA output of scintillator image from "pepper pot" above.

Fig. 4(b). The circular-hole pattern is obviously elongated in the defocussing plane and contracted in the focussing plane as an effect of the strong focussing channel. An analysis of the positions and widths of these spots gives complete information about the phase ellipse at that point for a single current pulse.

Initial analysis of this photograph gives good agreement with results from the standard slit-scanning methods used in SBTE. We are now planning to analyze this digitized information on the main LBL VAX computer and use the Dicomed digital display to examine this information in more detail.

THE NEUTRALIZED BEAM FOCUSING EXPERIMENT

A difficulty encountered in the experimental study of the Robertson plasma focusing lens is ensuring that the electrons be sufficiently cold. During the previous reporting period it was shown that grid neutralization yielded electrons with temperatures of about 40 eV. It was determined that having an electron temperature of about 1 eV would help make data interpretation easier as space charge effects would be minimized. This enhances the ability to distinguish the focusing effect due to the lens which is sought from residual space charge effects. The idea that was tried for achieving lower electron temperatures was to shoot the beam through a low temperature plasma.

A hot filamentary discharge was used to produce the plasma. Eight six-inch long, 20 mil tungsten filaments were placed around the beam axis, aligned parallel to the beam axis. They were placed about 1.25 meter downstream of the grounding grid of the ion gun. Argon is puffed onto the filaments, and a discharge voltage of from -50 volts to -300 volts is switched onto them. The gas breaks down due to impact of electrons that are emitted from the hot filament. A Langmuir probe was placed about 1 m from the filaments. The plasma density indicated was $\geq 8 \times 10^8$ cm^{-3} and the electron temperature was 2 eV.

The Cs^{+1} ion density is about 10^8 cm^{-3}. There is no confinement, so the plasma density near the filaments is higher than the above number. The plasma density is proportional to the amount of gas puffed into the system as is the time to re-evacuate the system. The maximum plasma density quoted above arises from the requirement that at least .5 pulse per minute

data acquisition is achieved. The pulse-to-pulse variation is at the 10 percent level when the plasma is on.

With this arrangement the beam density on axis was observed to increase by a 50 percent when the lens was turned on. Typical data appear in Fig. 5. The beam emittance was determined using envelope measurements and the spot size given by the 20 G case was within 30 percent of the best that could be expected.

It is now clear that the collective lens focuses the beam. However, some of the quantitative details are still not consistent. For example, saturation of the beam intensity on axis has not occured even at B = 40G. This should happen at about B = 15G if the theory based on Robertson's expression for the focusing strength is correct. Qualitatively, this problem is attributable to the fact that the neutralization of the beam becomes worse as the magnetic field is increased. Consequently greater space charge defocusing occurs. Unfortunately, no quantitative theory of this effect exists as yet.

Finally, when the plasma is on, a substantial fraction of the Cs^{+1} is converted to Cs^{+2}. We are in the process of trying to eliminate this problem. The addition of yet another variable into the beam dynamics is sure to obscure interpretation of the results.

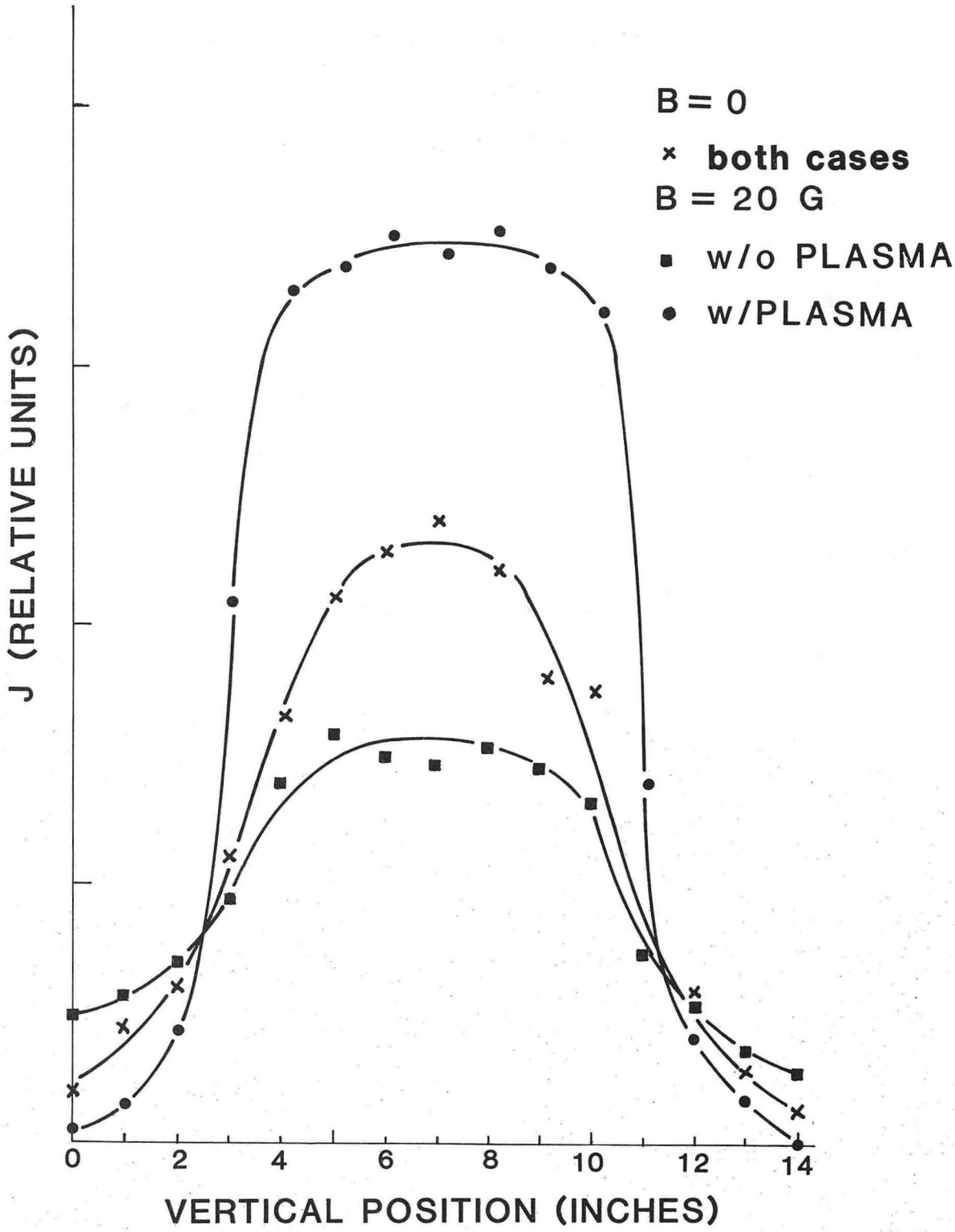

XBL 844-1620

Fig. 5. Beam Current Profiles at "Focus". These cases have equal incident current. A case with no neutralizing electrons has intensity small compared to the above data.

INDUCTION LINAC COMPONENT DEVELOPMENT

In an effort to reduce the costs of an induction linac driver, our ongoing program of component development has continued throughout this reporting period. The goal has been both to improve performance and reduce costs. There has been significant effort devoted to insulator development, switch tube development, and induction core development.

1. 200 kV Test Stand

In order to be able quickly to carry out high voltage testing of components for the Multiple Beam Experiment (MBE), in a realistic environment, we have modified an existing vacuum tank with a 200 kV Marx generator by adding on a large tank to the end. The intent of this arrangement is to have the interior of test insulators in vacuum and the exterior of the insulator surrounded by an insulating fluid such as Freon or SF_6.

We have also purchased a 200 kV DC hipotter to allow us to carry out DC high voltage testing as well as pulsed testing with the Marx generator. We have done only pulsed testing thus far, since the hipotter was delivered only in the last two weeks of the reporting period. The tests and results will be described in detail in the following sections.

2. Insulator Development

2.1 Polysil Model Insulators

The 5 large insulators, manufactured by Polytech, Inc. of Redwood City, CA, which were described in the last semi-annual report were all found to have major vacuum leaks due to failures in the casting and molding process. The Polysil mix shrank away from the mold. The mold was not flexible and

this created cracks in the final insulators. Attempts to patch the leaks on several of the insulators were unsuccessful.

Polytech then agreed to modify the mold, go to a more viscous Polysil mix and add a strengthening ring to the end flanges. This insulator assembly was fabricated and found to have 5 gross vacuum leaks. This insulator was then broken up by Polytech and the leaking regions examined. The cause was determined to be an insufficient bond between the stainless steel embedments and the Polysil. Because Polytech has had very good experience in bonding Polysil to copper and aluminum they feel that if they prepare the stainless steel properly they will succeed. It was therefore decided to try grit blasting the stainless steel followed by a 4 hour cleaning in a neutralizer tank. The stainless parts will be coated with the cyanoacrylate bonding agent just before casting the insulator. We expect to receive this test insulator assembly by May 1.

2.2. Re-X Insulators

It has recently come to our attention that General Electric makes a glass ceramic insulator material called Re-X which is mainly used for vacuum arc interrupter housings for electric utility industry service. The housings are made by assembling the stainless steel embedments in a mold which is then filled with the glass material and spun to form the vertical wall thickness. The cast parts are then annealed in an oven to form the glass into a ceramic. This appears to provide a very attractive package for induction linac insulator use, and we have purchased six of the largest size that GE makes (see Fig. 6 [BBC 841-237]).

We leak checked all of them and found only one which appeared to have a crack. We welded stainless steel conflat flanges to one of these and

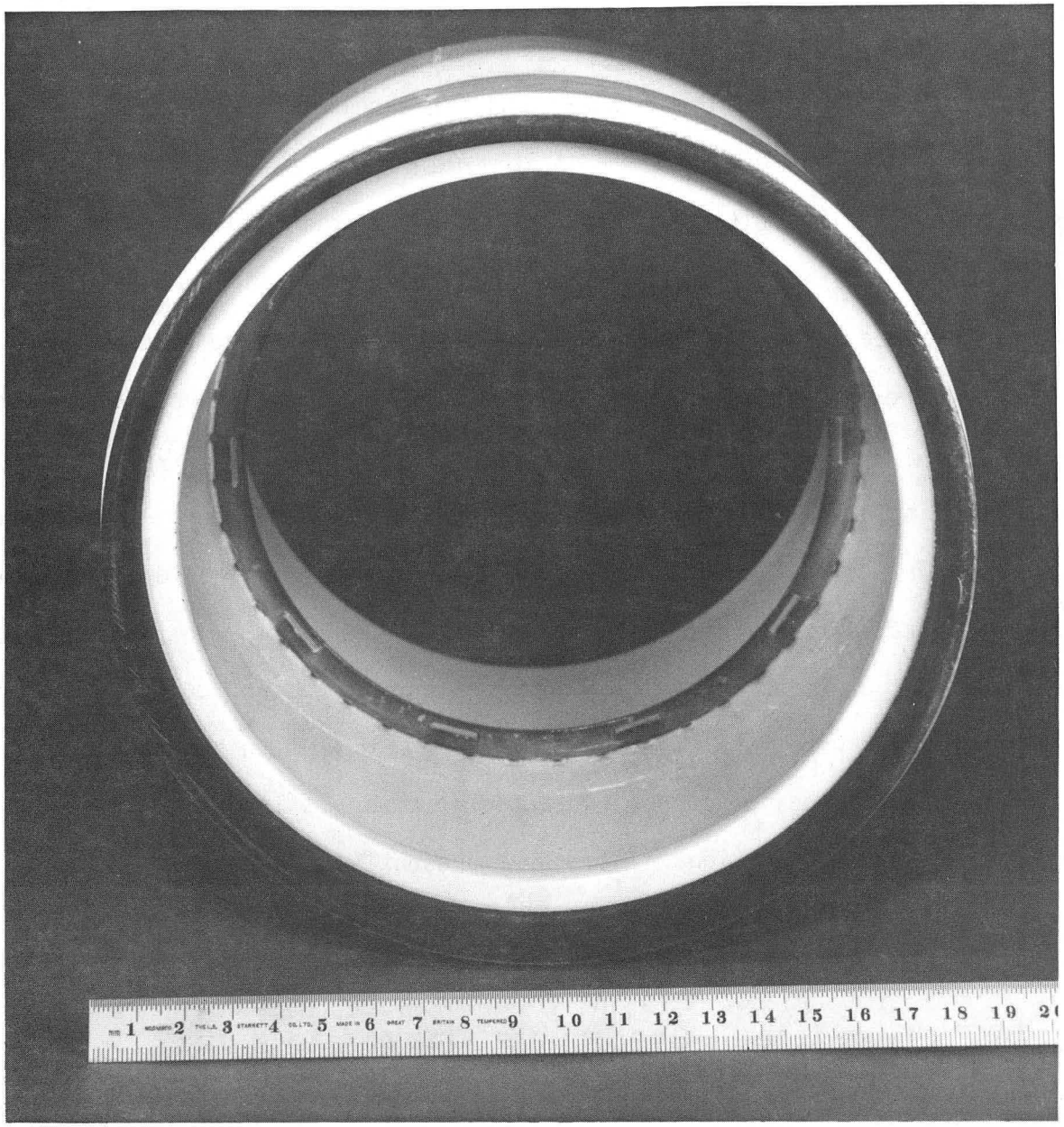

BBC 841-237

Fig. 6. Photograph of Re-X Insulator

measured the vacuum outgassing rate of the material after vapor phase cleaning in Freon and exposure to air for one hour. The results as shown in Fig. 7 indicate that the material is comparable to alumina in its unbaked and low temperature baked performance. This is an excellent result.

We then set the insulator up on the 200 kV test stand described previously and tested the voltage breakdown strength of the insulator with vacuum inside and SF_6 outside. In order to model induction linac service realistically we added skirts inside and outside to try to make the electric fields more nearly perpendicular to the insulator surface. We measured a full section of the insulator, 3 1/2 inches long, and then artificially "shortened" it by shorting out sections on the inside with a metal cylinder. The results are shown in Fig. 8. When considering these results it should be kept in mind that because the skirts were moved closer to reduce the insulator effective length, the electric field angle to the surface was not constant.

The results were sufficiently encouraging that we have begun discussions with GE to see if they would be interested in making a larger size insulator for accelerator applications. They are presently considering this and we expect to hear from them in the near future.

3. MBE Electrostatic Quadrupole Array

In order to gain information on the voltage breakdown in vacuum of an electrostatic quadrupole array which has been proposed for MBE, a mockup of a one beamlet array was made out of electropolished stainless steel. A photograph of the assembly is shown in Fig. 9 [BBC 841-225]. The rods are 2" in diameter and the aperture is 1 3/4".

After conditioning and several days of outgassing the vacuum gap held 130 kV without any glow discharge or x-ray production. The MBE quads are

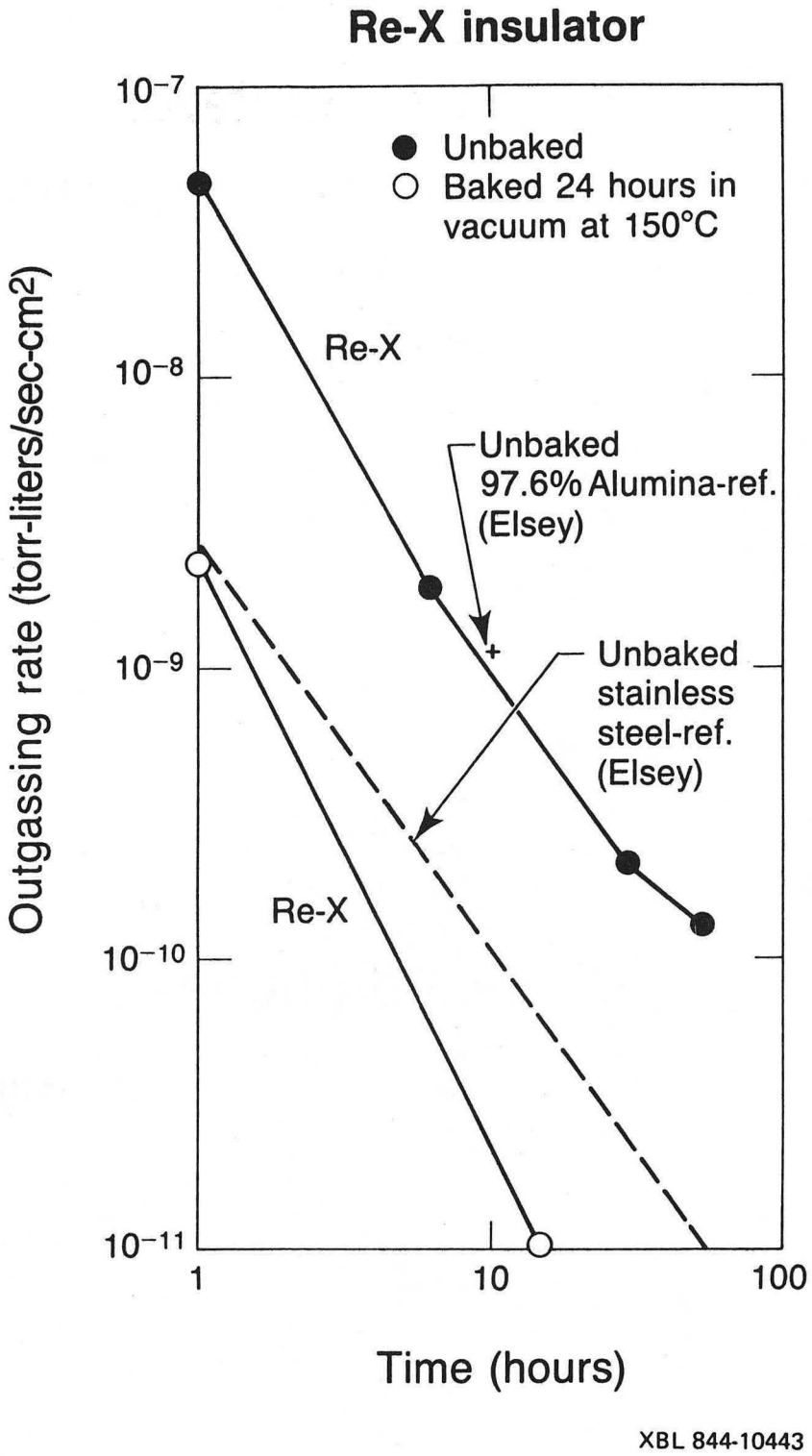

Fig. 7. Vacuum Outgassing Rate of Re-X Insulator

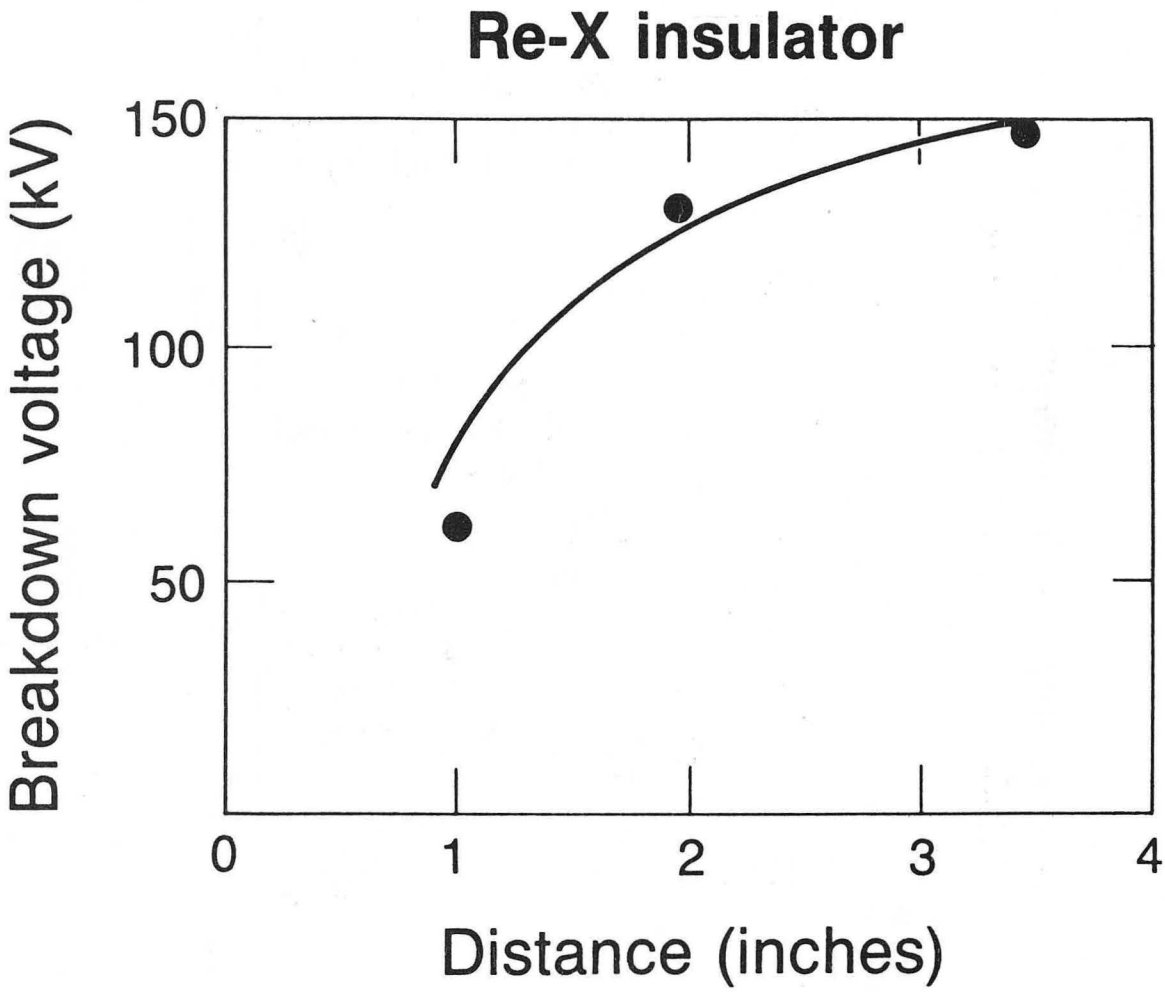

XBL 844-10444

Fig. 8. High Voltage Breakdown Strength of Re-X in Vacuum

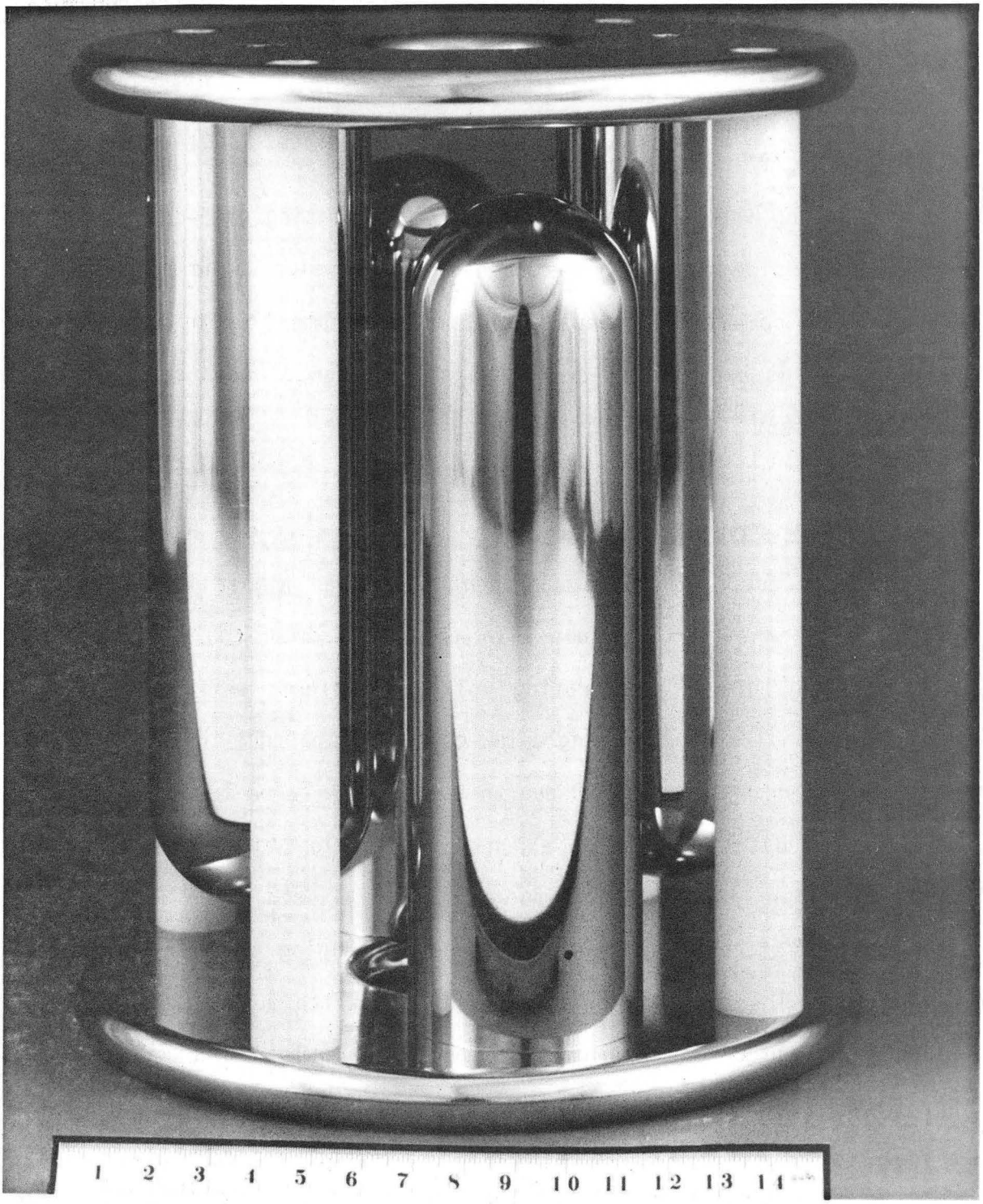

CBB 841-224

Fig. 9. MBE Electrostatic Quadrupole Array Mockup for High Voltage Testing

expected to hold 80 kV reliably. The next set of tests would involve directing an ion beam onto the electrodes, possibly using the SBTE, to see how much this degrades performance.

4. Outgassing Measurements

A program and the necessary hardware for automating data-collection on our vacuum outgassing measuring system has been developed and debugged for an HP 85 desktop computer. A report on this development is in preparation. This improvement is expected to speed the acquisition of data for insulator material development.

5. Switch Tube Development

The pulsers are one of the components where an almost ideal solution exists in the form of a hard tube with feedback, which could provide the desired specially shaped accelerating voltage waveforms while at the same time eliminating jitter, presenting a low coupling impedance to the beam, and allowing a smaller core to be used due to its ability to be turned on and off rapidly. Unfortunately it is too expensive an option and the alternatives all are lacking in one or more of the attributes listed. For long pulses, (greater than a microsecond), we have been developing an ignitron pulser because it is a low cost and efficient closing switch able to handle kiloampere currents and to pass coulombs of charge per pulse. The major shortcoming of ignitrons for this application, jitter, was reduced to 50 ns total in a developmental gridded tube, but in the first long test of a representative module, the grid eroded and caused tube failure at 5×10^6 pulses. This test was begun after successful operation of one tube driving a single induction core encouraged us to drive two cores in parallel. Now

we are life testing a one-core configuration again, and expect much more than twice as long life. For pulses below 1 μs, thyratrons are superior because of their shorter risetime and nanosecond jitter. Both of these low pressure gas discharge switches have to be protected from large reverse currents; in our case this is accomplished with a series saturated choke which comes out of saturation and presents a high impedance when the current reverses. This protective device more than doubles the circuit leakage inductance and slows down the rise and fall times. Because the ignitrons and thyratrons probably can be made to meet the near term requirements, other pulser options, such as spark gaps and magnetic modulators have not yet been seriously considered, the first because of their more powerful trigger requirements, and the second because of their long delay time.

We have recently obtained an ATA thyratron chassis from LLNL and are modifying it to allow us to see if the English Electric Valve CX 1538 thyratron used there could substitute directly for the failed ignitron. We also plan to investigate the possibility of using a second CX 1538 thyratron to carry the reverse current.

6. Metglas Core Tests

In collaboration with the Metglas Division of Allied Chemical Corporation we have been engaged in an ongoing program to engineer an induction linac core package which will provide maximum performance at a minimum price.

As part of this program we have looked at several Metglas 2605 SC core structures which are quite different than the "standard" one. The "standard" package involves dip coating the as-cast ribbon with a colloidal silica powder, winding it into a toroid and then annealing the finished toroid in an

applied magnetic field. The annealing process adds quite a bit to the cost of the finished core so Allied has made some cores from as-cast material which has been dip coated and spray coated (which is cheaper than dip coating) with colloidal silica powder. In addition, Allied fabricated a core which was annealed first and then rewound into a final core which was insulated with mylar. The results of core loss measurements done with our thyration pulser are shown in Fig. 10.

The losses are almost the same in all cases, but the ΔB swing is 1.1 T for the as-cast material, and 2.0 T for the annealed and rewound material. The as-cast material is clearly not very desirable for induction linac cores whereas the annealed and rewound material is essentially as good as the "standard" core package. We are now planning to do a similar set of tests on Metglas 2605 CO which contains 18 percent cobalt in place of some of the iron in the 2605 SC. Although 2605 CO material is 50 percent more expensive than 2605 SC it also gives 20 percent more ΔB swing in DC hysteresis loop measurements. Our pulsed measurements made several years ago confirm this flux swing result. Please note that we have quoted the "material only" values here. They have been corrected to 100 percent packing factor.

As an adjunct to this core loss measurement program we are planning to reactivate a thyratron pulser constructed several years ago to make measurements on these cores down to pulse lengths of a few hundred ns.

7. Surface Ionization Sources

Work on alumino-silicate ion sources continues. Na loaded zeolite has been prepared following a published recipe which involves mixing the zeolite with molybdenum powder and sintering. Thermal emission limits have been measured under these conditions and are found to be similar to those observed

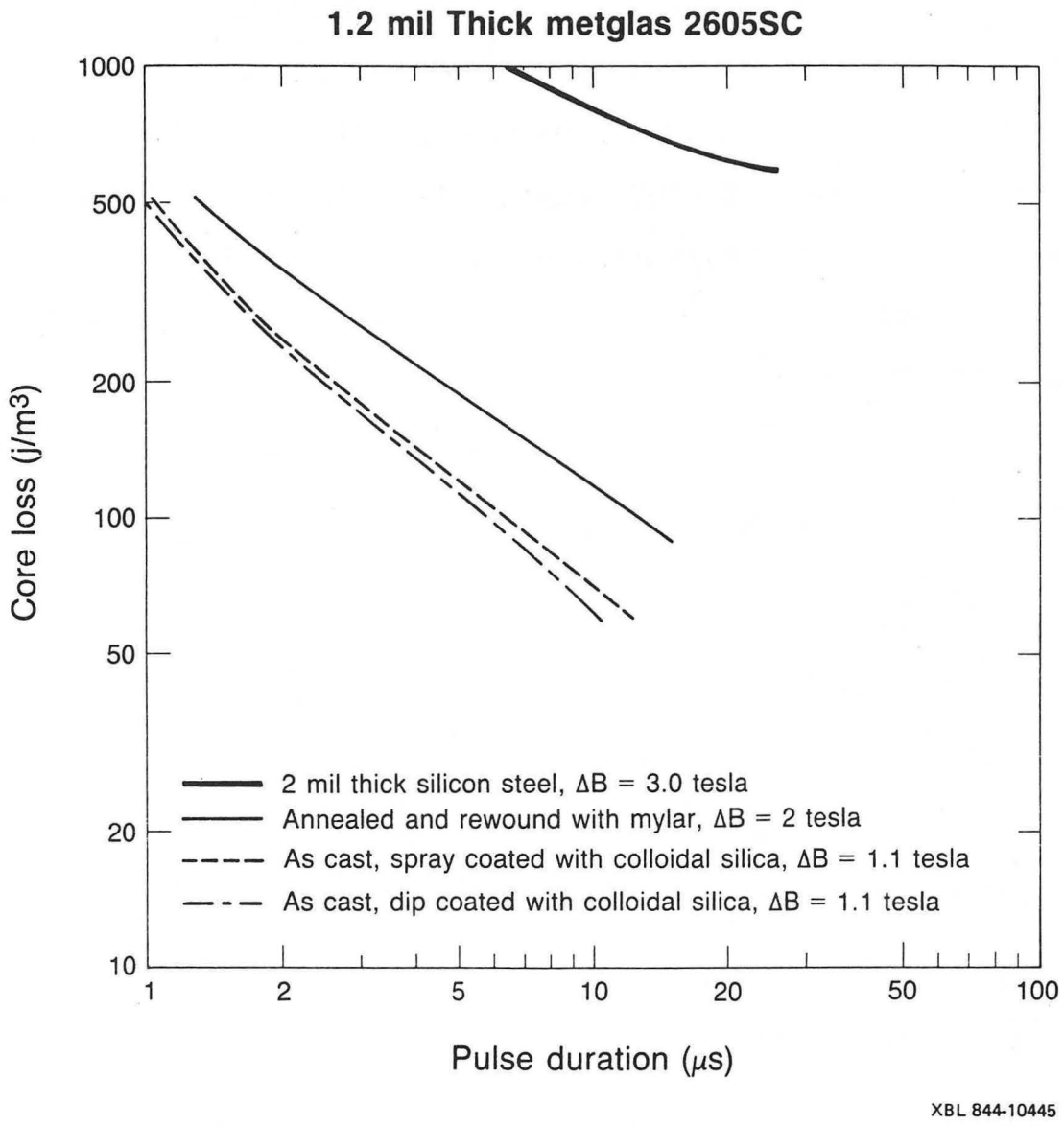

Fig. 10. Metglas 2605 SC Core Loss, Corrected to 100% Stacking Factor

from melted alumino-silicate. Variations up to a factor of five in the maximum emission are seen between local spots on the same emitter surface. The high emission spots achieve no more than 7 or 8 mA cm^2 of Na^+. More careful preparation may give uniform space charge limited emission from the sintered sources. If so, this technique will be used to prepare Cs^+ sources for the single beam experiment. Na^+ emission limits from alumino-silicates have not reached the desired values for the MBE design. An alternative approach of contact ionization on an oxygenated tungsten surface will be pursued in the next few months.

MULTIPLE BEAM EXPERIMENT (MBE)

The preceding Semi-Annual Report (LBL-16789/UC-21/HI-FAN-231, for the period through September 30, 1983) summarized the conceptual design studies performed for a High-Temperature Experiment (HTE) and referenced a Laboratory Report (HI-FAN-229) that provided some detailed data concerning the induction linac for that facility. Work throughout the current reporting period accordingly has now been directed to design of a Multiple-Beam Experiment (MBE), intended to test as many of the physics and engineering features of the HTE as are possible on a relatively small scale.

Attention is now sharply focussed on developing of a "Conceptual MBE Program Plan Report" for MBE by May 1984. The effort is intended to bring together the electrical and mechanical engineering designs into a compatible hardware example for MBE. Since the MBE apparatus will require a number of years for assembly, the incorporation of improvements in design as they occur are not at all precluded. A guiding test question in making MBE design and goal decisions is: "How does this relate to HTE "

In making engineering decisions, which are compromises among conflicting requirements, the need for sensitivity analyses of the consequences of departing from ideal choices has led to considerable theoretical activity.

It is recalled that the HTE visualized accelerating some 1.875 μcoulomb of Na^{+1} ions, divided amongst 16 beams, from a kinetic energy of 2 MeV to 125 MeV. The length of the injected beam was taken to be 25 m, and a compression factor of 0.4 led to a length of 10 m for the beam emerging from the linear accelerator. There is a recognized need for development of a high-quality source of Na^{+1} ions to serve as an injector with sufficient

intensity for these applications. Such developmental work is under way both at LANL and here, with frequent consultation between our Laboratories.

The MBE similarly would adopt 2 MeV as the injection energy. With an accelerator length of about 30 m, the final kinetic energy becomes limited to values somewhat less than 10 MeV (e.g., to ~ 7 MeV for ions in the center of the accelerated bunch), but it is intended that the acceleration fields shall attain values toward the end of the accelerator that are as great as the limiting values ($\langle \bar{E}_z \rangle \simeq 0.4$ MV/m) considered technologically suitable for the HTE. Some shortening of the pulse duration of course will occur during acceleration, and a moderate amount of spatial compression should also be demonstrable, both contributing to the effect of current amplification. The transverse-focusing lattice is intended to be of a design suitable also for that portion of a HTE accelerator wherein use of electrostatic quadrupole focusing would be appropriate.

The relatively short length of the MBE requires that the injected beam be short compared to the length of the accelerator if current amplification is to occur, and that, in consequence, the transportable <u>charge</u> in each of the 16 beam lines be considerably less than planned for the HTE. We seek, nonetheless, to have in the MBE a value of transportable <u>current</u> comparable to that intended for the HTE. The increased charge needed in HTE will be obtained by increasing the initial bunch length by a factor of three and is not considered to imply any essential physics or engineering uncertainties. Emphasis has been placed at present on a MBE design in which, for convenience and simplicity, the half-period of the focusing lattice is maintained constant throughout the length of the accelerator (L = 12 1/2 inch = 0.3175 m, with an occupancy $\eta = 1/2$). Such a design may be expected to be capable of transporting along the MBE accelerator a current that at injection is about

one-half that projected for the HTE, without exceeding the maximum envelope radius planned for the latter facility (~11 mm). By some reduction of the beam-electrode clearance in the comparatively short MBE device, moreover, currents substantially equal to those required in the HTE should become transportable.

When the ion to be accelerated in the MBE is taken to be Na^{+1} (desirable for practical achievement of desired target temperatures in the HTE, but <u>not</u> optimal for an inertial-fusion power-plant driver), then a convenient restriction of injected pulse duration to values no less than 2 μsec ($\ell_0 \simeq 8.2$ m, for Na^{+1} at 2 MeV) results in the development of some troublesome characteristics during the course of acceleration in the MBE. Specifically, there necessarily develops a very pronounced difference of speed between particles at the head and tail of the beam when passing any given point, and this feature introduces, in turn, substantial restrictions on the beam intensity that can be stably transported. For this reason we have included in our MBE studies examination also of the more conservative performance expected with beams of K^{+1} ions ($\ell_0 \simeq 6.3$ m) and Cs^{+1} ions ($\ell_0 \simeq 3.4$ m). For these latter ions the realization of ion sources of useful intensity may, in fact, be more readily achieved, and use of such ions accordingly may be expected to be convenient for much of the experimental work.

THEORY

1. Design Questions for MBE

At the present time a substantial body of data has been computed concerning the electric-field characteristics of various specific configurations considered for the quadrupole focusing elements, and dynamical computations of the individual-particle and collective motion of ions in such fields are in progress. In parallel with such detailed studies of beam dynamics, a strong mechanical engineering activity is under way to study the possible physical lay-outs for the induction cores and focusing elements, and their electrical excitation.

During early work on such layouts and on integration of the components into a complete system a number of topics requiring analytic and/or digital calculations has received attention; more, no doubt, will appear as the work progresses. For example, a succession of basic linac dynamics calculations has been made to examine effects of various constraints suggested by consideration of alternative physical layouts. These suggested constraints have included:

(a) constant focusing-period length along the linac for mechanical modularity, hence simplicity;

(b) constant applied focusing voltage along it for electrical simplicity, which later was found to be of little cost consequence; and

(c) smaller ratio of focusing electrode radius to beam clearance radius, with a corresponding reduction of transverse beam separation; this would allow the 16-beam focussing array to

be shrunk in transverse dimensions which, in turn, would permit the insulator and inner diameter of the cores to be reduced and, hence, lead to cost savings.

Some of these suggested changes, taken together with previously established desired beam and beam-clearance radii, would reduce the current that could be transported; additional calculations, using different values of some parameters (e.g., σ_0 at the beam bunch head and focusing packing-fraction), were made to determine how much of such reductions of capability might be recovered.

A number of calculations were made to study effects of departures in realizable dimensions and field shapes from simple idealized forms, to identify unacceptable effects, or to estimate tolerances required to make the effects acceptable. Examples of such work are briefly summarized below.

1. The effects on beam clearance of transverse misalignments of focusing-element modules were studied, and tolerances estimated. The most serious misalignments have Fourier space components with wavelengths comparable to the free-oscillation wavelength $4\pi L/\sigma_0$ (L = lattice half-period), as modified by image-charge force, which exist coherently for several wavelengths. There will be a range of such critical wavelengths, depending on the range of σ_0 between bunch head and tail, which in turn will vary with beam intensity. It appears that a tolerance of order 0.01 inch at the resonant wavelength is required to limit coherent beam displacements to 1 mm.

2. The effects of sixth-harmonic azimuthal components in focusing fields, arising from departures of the ratio of focusing electrode radius to beam clearance radius from the optimum value, have been studied by simulation calculations. The present design radius for the MBE focussing electrodes (2.406 cm) was chosen to minimize the magnitude of non-linearities of the focussing field. Reducing the electrode radius would reduce the size, and therefore the cost, of the experiment, at the expense of introducing non-linearities. A particle simulation code developed by I. Haber of NRL was used to study the effect of these fields on the transverse stability of the beam. The magnitude of the non-linear focussing forces was determined using an electrostatic relaxation code, and the field thus calculated was used in the simulation.

A study of the effects of the perturbing potential ($\propto r^6 \cos 6\theta$) introduced by halving the electrode radius showed stability of the beam, with no emittance growth, for a beam centered in a quadrupole channel. However, emittance growth was seen for off-center beams, of magnitude ~ 40 percent in 25 periods for a displacement of 5.5 mm (displacement in the "x" direction at the center of an x focussing lens) and ~ 10 percent in 50 periods for a displacement of 2.75 mm. For electrodes of radius equal to 3/4 of the design radius, with Δx = 5.5 mm, the emittance growth was ~ 10 percent in 50 periods. Beam dynamics considerations therefore support the original choice of radius.

Investigation of the effect of non-linearities using the simulation continues. Work is presently under way to determine the effect on the beam of end effects, which occur where positive and

negative arrays do not overlap longitudinally, of image forces, and of non-linear forces due to the asymmetry of the MBE array, as seen by a single beam. The scarcity of Class VI computer time continues to restrict the scope and thoroughness of such studies.

3. Estimates have been made of the total electric field of the several beams in the spaces between focusing regions, and of the transverse displacements of individual beams this field may produce. Two different analytic field calculations, using boundary conditions approximating the actual geometry, were evaluated numerically to obtain the fields. For initial beamlet currents of order 100-200 mA the displacements are of order 1 mm or less, and could be further reduced, if necessary, by introducing additional conducting surfaces.

4. Actual applied accelerating fields will differ from the smooth waveform shapes derived from basic dynamics computations in two respects; they are applied stepwise in separated gaps rather than continuously, and the idealized shapes are approximated by a succession of finite steps. The effects of these differences are being studied using a new computer program, which will also be used to examine effects of switch misfires, timing jitter, and other imperfections. Information derived from these computations also leads directly to more detailed consideration of the subdivision of accelerating core elements within the different core modules.

2. Calculation of Non K-V Equilibrium Properties

The Kapchinskij-Vladimirskij (K-V) distribution of transverse coordinates and momenta is known to become unstable at high intensity, even in the limit of continuous focusing. This limit is an adequate approximation for $\sigma_0 < 60°$, and the matched envelope is round and constant in time, with flat-top current density. Simulation has previously shown that unstable behavior of such a beam quickly quenches and a new, stable distribution results. The rms emittance of the new distribution is slightly smaller than that of the original K-V. This behavior is predicted by an analytical calculation based on the assumptions: conservation of net current, conservation of net transverse energy, and application of the equilibrium virial relation for axisymmetric distributions. The rms emittance of the K-V distribution is a maximum subject to these constraints.

In order to predict the actual emittance of the final (stable) distribution, a specific model distribution function is adopted. We have examined the two classes

$$f_1 = N_1 H\,(E_1 - E) \quad ,$$

$$f_2 = N_2 (E_2 - E)\; H(E_2 - E) \quad ,$$

where E is a particle's transverse energy (kinetic plus potential) and H denotes the Heaviside function. These distributions satisfy the sufficient conditions for stability $df/dE < 0$ [which is violated by the K-V: $f_0 = N_0 \delta(E_0 - E)$]. The coefficents N_1, E_1, N_2, E_2 are determined from the K-V parameters by the constraints on current and net energy.

The case f_1 is analytically soluble, with charge density

$$\rho(r) \propto \left[1 - I_0(kr)/I_0(ka)\right]$$

where I_0 is the modified Bessel function and K is a constant depending on initial tune depression. In the limit of very depressed tune ($\sigma/\sigma_0 \to 0$) the final emittance (ε) is

$$\frac{\varepsilon}{\varepsilon_{KV}} = 1 - \frac{1}{12}\left(\frac{\sigma}{\sigma_0}\right)_{KV} ,$$

while the edge radius (a) increases according to

$$\frac{a}{a_{KV}} = 1 + \frac{1}{2}\left(\frac{\sigma}{\sigma_0}\right)_{KV}$$

The analysis of f_2 has been achieved by an iterative numerical integration, [a non-linear boundary-layer problem is posed]. Initial (K-V) tune ratios have ranged from $\sigma/\sigma_0 = 1$ to .07, with maximum emittance reduction of 1.5 percent occurring at $\sigma/\sigma_0 \approx 0.4$. As $\sigma/\sigma_0 \to 0$, the variation is found to be

$$\frac{\varepsilon}{\varepsilon_{KV}} \cong 1 - (.049)\left(\frac{\sigma}{\sigma_0}\right)_{KV} .$$

These numbers are consistent in magnitude with simulation results.

PUBLICATIONS

LBL-16789 (HI-FAN-231)	HIF Staff	Heavy Ion Fusion Year-End Report April 1, 1983 - September 30, 1983 (12/83)
LBID-859 (HI-FAN-232)	A. Warwick	Emission Limits for Na^+ Ions from Alumino-Silicate Surface Ionization Sources (1/84) (In progress)
HI-FAN-233	W.B. Herrmannsfeldt	MBE Alignment (12/83)
HI-FAN-234	Edward P. Lee	Memorandum/Herman A. Grunder: Heavy Ion Fusion Simulations (12/83)
(HI-FAN-235)	R.K. Cooper P.L. Morton P.B. Wilson D. Keefe A. Faltens	Linac Technology For Free-Electron Lasers. Journal de Physique, Volume 44, Colloques Number 1
LBL-16996 (HI-FAN-237)	D. Keefe	Heavy Ion Drivers for Inertial Confinement Fusion Proc. IEEE 10th Fusion Energy Symposium, Philadelphia, PA, Dec. 5-9, 1983
LBL-17250 (HI-FAN-238)	A. Faltens	Induction Linac Plans (INS International Symposium on Heavy Ion Accelerators and their Applications to Inertial Fusion, Tokyo, Japan, Jan. 23-27, 1984.)
LBL-17255 (HI-FAN-239)	D. Keefe	Review of Induction Linac Studies (INS International Symposium on Heavy Ion Accelerators and their Applications to Inertial Fusion, Tokyo, Japan, Jan. 23-27, 1984.)
LBL-17256 (HI-FAN-240)	W. Chupp A. Faltens E.C. Hartwig D. Keefe C.H. Kim C. Pike S.S. Rosenblum M. Tiefenback D. Vanecek A.I. Warwick	A High Current Heavy Ion Beam Transport Experiment at LBL (INS International Symposium on Heavy Ion Accelerators and their Applications to Inertial Fusion, Tokyo, Japan, Jan. 23-27, 1984.)

LBL-17561 (HI-FAN-247)	C. Kim	Beam Experiment Programs in the USA (INS International Symposium on Heavy Ion Accelerators and their Applications to Inertial Fusion, Tokyo, Japan, Jan. 23-27, 1984.)
LBL-17197 (HI-FAN-241)	A.I. Warwick D. Keefe W. Herrmannsfeldt	Heavy Ion Accelerators as Drivers for Inertial Confinement Fusion (1984 Annual Meeting of the American Nuclear Society, New Orleans, LA, June 3-8, 1984)
LBID-880 (HI-FAN-242)	W.B. Ghiorso S.S. Rosenblum	An Automated System for Envelope and Emittance Measurement (3/84)
LBID-895 (HI-FAN-244)	E.P. Lee	The Effect of Long-Wavelength Distortions in a Beam Transport Lattice (3/84)
HI-FAN-245	V. Brady	Harmonic Analysis of Electrostatic Potential due to an Array of Round Rod Quadrupoles (3/20/84)
HI-FAN-246	A. Faltens L.J. Laslett	Permanent Magnet Quadrupoles in a Periodic Array (3/21/84)
HI-FAN-248	Victor Brady	Summary of CRAY Computer Runs Using Irving Haber's Program for Simulating Space Charge Effects in the Transverse Plane. (3/26/84)
HI-FAN 250	Victor Brady	Calculation of Aperture Ratios in One Dimension for Single Particle Motion in a Periodic Magnetic-Quadrupole Lattice with no Space Charge Present April 28, 1983. (4/84)

H.I.F. STAFF ROSTER

Denis Keefe

Robert T. Avery
Clarence Chavis
Warren Chupp
Edwin R. Edwards
Andris Faltens
Edward C. Hartwig
Charles H. Kim
Edward J. Lofgren
John Meneghetti
Chester D. Pike
Stephen S. Rosenblum
Gerald L. Stoker
Michael Tiefenback
David Vanecek
Anthony Warwick

Lloyd Smith

Joseph Bisognano
Victor Brady
Christine Celata
D. L. Judd
Geoffrey Krafft
L. Jackson Laslett
Edward P. Lee

Thomas J. Fessenden, LLNL

William B. Herrmannsfeldt, SLAC

HALF-YEAR REPORT: DISTRIBUTION LIST

Allied Chemical Corporation

Carl Smith

Argonne National Lab.

Thomas A. Fields
Ronald Martin

University of Arizona

R. Morse

Batelle

John Hartman

Bechtel

W. Allen

Brookhaven National Lab.

Mark Barton
Alfred Maschke

C.E.A. Bruyeres-le-Chatel

R. Dei-Cas

University of Calif., Irvine

Norman Rostoker

University of Calif., Riverside

Robert Poe

Cornell University

John Nation
Ravi N. Sudan

DARPA

Richard Gullickson
Joseph Mangano

Department of Energy

DP-OIF

Sheldon L. Kahalas
L. Killion
R. Schriever
Marshall Sluyter
Col. Charles Whited

ER

Terry Godlove
James S. Kane
Richard Kropschot
James Leiss
Gerry Peters
David F. Sutter
Alvin Trivelpiece, Dir.,
Office of Energy Research
William Wallenmeyer

DoE San Office

Rudolf Bredderman
Dennis Neely

E.P.R.I.

Robert Scott

Fermi National Accelerator Lab.

Frank T. Cole
Fred Mills
Lee Teng

GANIL

P. Lapostolle

GSI

R. Bock
D. Boehne
I. Hofmann

University of Illinois

G. Miley
Joseph Verdeyen

Institute for Nuclear Study

Y. Hirao

KMS Fusion, Inc.

Alex Glass
Michael J. Monsler

Kanazawa University

S. Kawasaki

Lawrence Berkeley Laboratory

R. Avery, 46/189
K. Berkner, 50/149
J. Bisognano, 47/112
W.W. Chupp, 47/112
T. Elioff, B46B
A. Faltens, 47/112
T. Fessenden, 47/112
A. Garren, 47/112
H. Grunder, 50A/4119
E. Hartwig, 47/112
E. Hoyer, 46/187
E. Hyde, 50A/4133E
R. Johnson, 50A/4119
D. Judd, 47/112
D. Keefe, 47/112
C. Kim, 47/112
M. Krebs, 50A/4112
W. Kunkel, 4/230
G. Lambertson, 47/112
L.J. Laslett, 47/112
E.P. Lee, 47/112
E. Lofgren, 47/112
J. Meneghetti, 46/161
J. Peterson, 47/112

Lawrence Berkeley Laboratory (cont'd)

S. Rosenblum, 47/112
A. Sessler, 4/230
D. Shirley, 50A/4113
L. Smith, 47/112
D. Vaughan, 50/149
A.I. Warwick 47/112

Lawrence Livermore Laboratory

Richard J. Briggs, L-321
John L. Emmett, L-488
John Holzrichter, L-481
William Krupke, L-488
Jim Mark, L-477
John Nuckolls, L-477

Lockheed

John Siambis

Los Alamos National Laboratory

Roger Bangerter
Ihor Bohachevsky
Richard Cooper
Robert Jameson
Don Kerr
D. Neuffer
Roger B. Perkins
Steve Rockwood
Henry Rutkowsky
Richard Stokes
Don Swenson
Tai-Sen Wang

University of Maryland

Martin Reiser
Derek Tidman

Max Planck Inst. fur
Plasma Physik Garching

Arnulf Schluter

Maxwell Laboratories

Library

National Bureau of Standards

S. Penner
M. Wilson

National Science Foundation

Edward Knapp, Director

Naval Research Lab.

Steven Bodner
T. Coffey
Irving Haber
Philip Sprangle
Peter Turchi

Occidental Research Corp.

Wyn Salisbury

Osaka University

T. Mochizuki
C. Yamanaka

Universita di Padova

A. Pascolini
M. Pusterla

Physical Dynamics

G. H. Gillespie

Physics International

Library

RAFAEL

Joseph Shiloh

Rutherford Laboratory

John D. Lawson
Chris Pryor

Sandia Laboratories

Everet H. Beckner
Don Cook
Glenn Kuswa
Tom Martin
J.P. Vandevender
Gerold Yonas

Soka University

Tetsuya Saito

SOREQ Nuclear Research Center

A. Sternlieb

SLAC

William Herrmannsfeldt, Bin 26
Burton Richter, Bin 7

TRW

J. Gordon
Z. Guiragossian
J. Maniscalco
W. Steele

Westinghouse

M. Nahemow
E. W. Sucov

University of Wisconsin

G. Kulcinski
G. Moses
R. Peterson

This report was done with support from the Department of Energy. Any conclusions or opinions expressed in this report represent solely those of the author(s) and not necessarily those of The Regents of the University of California, the Lawrence Berkeley Laboratory or the Department of Energy.

Reference to a company or product name does not imply approval or recommendation of the product by the University of California or the U.S. Department of Energy to the exclusion of others that may be suitable.

TECHNICAL INFORMATION DEPARTMENT
LAWRENCE BERKELEY LABORATORY
UNIVERSITY OF CALIFORNIA
BERKELEY, CALIFORNIA 94720